Vol. 48, No. 1 (2026) 117-130, DOI: 10.24874/ti.2019.09.25.12

Tribology in Industry

www.tribology.rs

RESEARCH

Development and Characterization of Al6061-Rice Husk Ash and Al6061-Fly Ash Composites for Tribological Brake Disc Applications

S. Suresh Kumar[a,*], A.S. Bindhu[b], V.S. Niranjan Kumar[c], H.S. Manjunatha[b], K. Praveen Kumar[d], Pavankumar Ravikumar[b]

[a]*Department of Mechanical Engineering, The National institute of engineering, Mysuru, Karnataka, India,*
[b]*Department of Mechanical Engineering, SJCE, JSS Science and Technology University, Mysuru, Karnataka, India,*
[c]*Department of Mechanical Engineering, ATME College of Engineering, Mysuru, Karnataka, India,*
[d]*Department of Mechanical Engineering, Government Engineering College, Kushalnagara, Karnataka, India.*

Keywords:

Al6061
Brake disc
Fly ash
Rice husk ash
Tribology
XRD

* Corresponding author:

S. Suresh Kumar
E-mail:
sureshkumarsiddaiah@gmail.com

Received: 9 September 2025
Revised: 11 October 2025
Accepted: 15 December 2025

A B S T R A C T

The increasing demand for lightweight and sustainable automotive components has driven significant research into alternative materials for brake disc systems, as conventional cast iron discs contribute to excessive vehicle weight, reduced fuel efficiency, and higher emissions. This study develops and evaluates aluminum matrix composites (AMCs) based on Al6061 reinforced with rice husk ash (RHA) and fly ash (FA) to assess their mechanical and tribological performance for brake disc applications. Six composite samples containing 2, 4, and 6 wt% of RHA and FA reinforcements were fabricated using vortex-assisted stir casting, and their properties were characterized following ASTM standards (tensile: E8M-13a, hardness: E384, wear: G99-95). Wear optimization and statistical analysis were performed using Taguchi L9 orthogonal design, ANOVA, and regression modeling, with low R^2 values (18.95% for FA, 20.24% for RHA) supporting the Taguchi approach that emphasizes parameter ranking. The composite containing 6 wt% hybrid (RHA+FA) reinforcement exhibited optimal performance, showing a 10–15% improvement in hardness, approximately 20% reduction in wear rate, and a stable coefficient of friction between 0.35 and 0.40—values comparable to those of cast iron. Overall, the developed Al6061–RHA–FA composite offers a 40–60% reduction in weight compared to traditional brake discs while maintaining excellent thermal stability and wear resistance, presenting a sustainable, high-performance alternative that utilizes agro-industrial waste for automotive applications.

1. INTRODUCTION

The urgent need to reduce vehicle weight without sacrificing safety has driven research into advanced materials for automotive components. Brake discs, significant contributors to unsprung mass, affect ride quality, fuel efficiency, and handling. Traditional cast iron discs, though durable and thermally stable, add weight that can increase fuel consumption by up to 15% and reduce braking responsiveness during rapid deceleration [1]. This enhances heat dissipation, reducing thermal fade and maintaining braking performance under repeated braking [2].

Aluminum matrix composites (AMCs) have emerged as promising alternatives (Figure 1), offering 40–60% weight reduction and twice the thermal conductivity of cast iron [3]. Key material properties comparing Al-MMCs and cast iron discs are summarized in Table 1.

Table 1. Material properties of Al-MMCs and cast iron brake disc [3].

Property	Al-MMCs	Cast Iron	Units
Tensile Strength	484	207	MPa
Yield Strength	437	330	MPa
Young's Modulus	114	114	GPa
Poisson's Ratio	0.33	0.27	–
Density	2.822	7.20	g/cm^3
Thermal Conductivity	140.2	45.0	W/m·K
Thermal Expansion Coefficient	2.3×10^{-5}	1.2×10^{-5}	/K
Specific Heat	800	510	J/kg·K

Aluminum Brake Disc Cast Iron Brake Disc

Fig. 1. Brake disc material.

In addition to weight and thermal management advantages, brake discs must satisfy rigorous mechanical and tribological requirements. Tensile strength determines a disc's capacity to withstand tensile stresses induced by clamping forces and thermal gradients, while surface hardness governs resistance to abrasive and adhesive wear caused by brake pad contact. Wear resistance is especially critical: excessive material loss can alter disc geometry, impair pad contact uniformity, and increase vibration and noise. Bench-scale pin-on-disc tests (Figure 2.) reveal that a 20% improvement in wear resistance can extend service life by up to 50%, reducing maintenance costs and downtime.

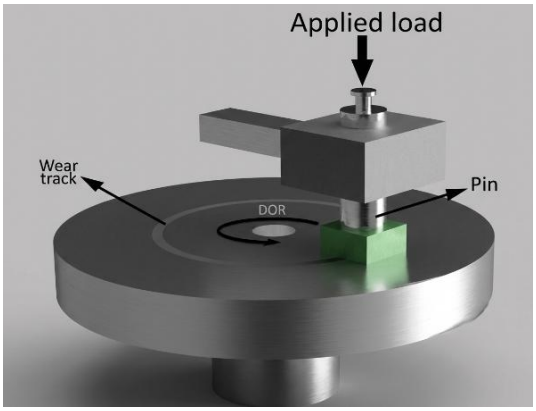

Fig. 2. Pin-on-Disc Wear Test Schematic

The application environment for brake discs also emphasizes fatigue resistance under thermal cycling. Braking events generate rapid temperature fluctuations - often from ambient to over 200 - 500 °C within seconds (Figure 3.) - creating thermal stresses that can initiate microcracks. Fatigue life analysis indicates that materials capable of sustaining more than 10,000 thermal cycles without crack initiation ensure reliable performance in commercial and high-performance vehicles. Aluminum alloys, when suitably reinforced, can meet these fatigue life criteria while maintaining lightweight characteristics [4].

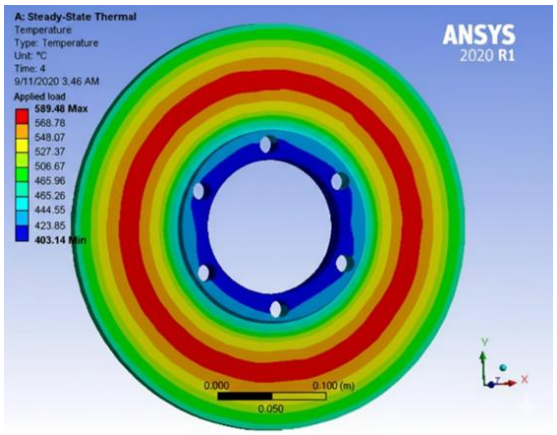

Fig. 3. Brake Disc Thermal Cycling Simulation

Beyond mechanical needs, environmental concerns push toward sustainable materials and manufacturing. Using industrial byproducts and agro-waste reinforcements supports circular economy principles by reducing landfill waste and lowering composite embodied energy by up to 30% compared to synthetic materials. Brake discs are typically fabricated through cost-effective casting with controlled particle incorporation, enabling scalable production. Quality control via non-destructive testing and mechanical assessments, combined with finite element modeling of brake dynamics, optimizes material and design choices.

This study evaluates aluminum composites for brake disc applications by systematically linking composite composition, processing parameters, and performance metrics like tensile strength, hardness, and wear resistance to international standards.

The goal is to

- Fabricate and compare Al6061 composites reinforced with RHA and FA.
- Evaluate tensile, hardness, and wear performance.
- Optimize wear parameters using Taguchi analysis.
- Validate findings for real brake disc application.

Although numerous studies have investigated RHA and FA separately as reinforcements in Al6061 composites, few have explored a direct comparison under identical process parameters. Even fewer have optimized the reinforcement content to achieve a balanced improvement in both mechanical and tribological properties. Moreover, the effects of hybrid RHA–FA combinations on wear resistance and strength remain underreported. This study addresses these gaps by systematically fabricating and analyzing Al6061 composites with varying wt% of RHA and FA and applying Taguchi optimization to assess performance

2. LITERATURE REVIEW

The research further explores aluminum matrix composites reinforced with agro-industrial wastes such as rice husk ash (RHA), providing lightweight, high-strength, and wear-resistant materials. This overview highlights advances in AMC fabrication using RHA, fly ash, and silicon carbide (SiC), emphasizing sustainable processing, enhanced mechanical and tribological properties, and alignment with circular economy goals through the valorization of waste materials.

Yadav et al. [5] reviewed aluminum matrix composites (AMCs) reinforced with rice husk ash (RHA), highlighting its benefits in enhancing hardness, tensile strength, and wear resistance in AA6061 alloys through scalable stir casting. Increasing RHA shifted wear from adhesive to abrasive, improving automotive applicability. Bahl's [6] review covered fiber-reinforced MMCs, focusing on manufacturing methods and fiber–matrix interface bonding, crucial for strength and durability in aerospace and automotive sectors. Orjuela et al. [7] examined polymer composites of rice husk (RH) with polypropylene and polyethylene, using sulfur-silane coupling agents to enhance bonding, reducing flammability and improving thermal stability for automotive and construction use. Musa et al. [8] studied rice husk briquettes as fuel for melting metals in crucibles, finding efficient combustion and pollution control, supporting rice husk briquettes as a sustainable alternative to fossil fuels.

Sangale et al. [9] investigated AA6061 aluminum reinforced with RHA by stir casting, showing hardness increases with RHA content at 4%, 8%, and 12%, and further gains after heat treatments, especially quenching. Nurazzi et al. [10] reviewed chemical treatments of natural fibers improving fiber-matrix compatibility and thermal stability in polymer composites, covering thermoplastic, thermoset, and hybrid matrices. Alaneme et al. [11] researched aluminum hybrid composites reinforced with RHA and alumina via double stir casting, noting corrosion resistance highest in alumina-only composites and increased wear rate with higher RHA, causing a shift in wear mechanisms. Ravi Kumar et al. [12] explored hybrid aluminum composites with fly ash and RHA via stir casting, finding that balanced reinforcement (~10 wt.% each) improved tensile strength, hardness, and wear resistance, while excess fly ash lowered performance; magnesium addition improved particle wettability. Siswanto et al. [13]

presented an eco-friendly fabrication of aluminum composites using RHA and scrap aluminum via evaporative casting, showing that higher pouring temperatures (650–750 °C) and RHA content (up to 10%) enhance hardness and fluidity while reducing porosity, supporting circular economy principles through waste valorization. Hasan et al. [14] reviewed aluminum composites with up to 9 wt.% RHA via sand casting, reporting linear increases in tensile strength (up to 84% increase in yield strength), hardness, and impact energy (up to 70% increase), but noted brittleness with higher RHA, requiring optimized processing. Devi Chinta et al. [15] enhanced aluminum properties by reinforcing with RHA and SiC via stir casting, demonstrating improved hardness and compression strength with better particle dispersion and controlled inert atmospheres to prevent oxidation; microstructure analysis showed grain growth contributing to property trends.

Reddy et al. [16] fabricated Al6061-T6 composites using RHA and Bakelite via stir casting, reporting ~15% higher wear resistance and ~8.5% increased hardness over the unreinforced alloy, highlighting the dual benefits of agro- and polymer-waste reinforcements. Raj et al. [17] investigated Al6061 with 0–8 wt% fly ash and graphite, optimized using Taguchi analysis. The 6 wt% FA composite showed the lowest wear rate, with FA content contributing ~34% to wear reduction, confirming its effectiveness for wear-resistant automotive parts.

Samuel et al. [18] applied two-step stir casting to Al–Cu alloys reinforced with 1–4 wt% RHA, achieving over a twofold hardness increase (from ~54.2 HV to 122.7 HV) and significant wear resistance in dry and acidic conditions, supporting RHA's use in harsh environments. Narendran et al. [19] studied AA6082 reinforced with eggshell and fly ash; a 6% ES–4% FA hybrid raised tensile strength from ~141 MPa to ~193 MPa and reduced the coefficient of friction from 0.489 to 0.265. Sliding distance was found to be the dominant factor influencing wear, verified through response surface methodology. These works collectively affirm the role of agro-industrial reinforcements in enhancing strength, hardness, and wear performance of Al6061-series composites for automotive applications.

Research demonstrates that RHA significantly enhances hardness, tensile strength, wear resistance, and impact absorption in aluminum alloys like AA6061 and AA7075 through methods such as stir casting and evaporative casting. Optimized particle dispersion and processing are vital to prevent brittleness and porosity, while reinforcements like fly ash can further improve properties if used judiciously. Improved interfacial bonding via coupling agents enhances performance for automotive, aerospace, and construction applications. Overall, these studies validate RHA and fly ash as a valuable, eco-friendly reinforcement for high-performance aluminum composites.

3. MATERIALS AND METHODS

3.1 Materials

Aluminium is widely used in engineering due to its exceptional properties including corrosion resistance, thermal and electrical conductivity, and high strength-to-weight ratio. The matrix material used in this experiment is Al 6061 alloy, renowned for its high specific strength, corrosion resistance, stiffness, and wear resistance, making it ideal for structural and automotive applications. [20]. Al6061 alloy was procured from Ananya Fluoropolymer, Bangalore, with chemical composition conforming to the ASTM B308 standard for Al 6061.

Rice husk ash (RHA) particles were utilized as the primary reinforcement Rice husk ash (RHA) (60 μm) was used as the primary reinforcement material (Figure 4.). RHA is an agricultural by-product representing 20% of rice production weight, processed through controlled combustion at 600-700°C to produce silica-rich ash. The chemical composition (Table 2) shows predominantly SiO_2 content (90-93%), providing excellent reinforcing properties. [21]. Fly ash (FA) (50 μm) served as secondary reinforcement for the composites (Figure 5). FA is a coal combustion by-product from thermal power plants, consisting primarily of SiO_2, Al_2O_3, and Fe_2O_3 with 10-100 micron particle sizes. The chemical composition is shown in Table 3.

Fig. 4. Rice husk ash.

Fig. 5. Fly ash.

Table 2. Chemical composition of rice husk ash.

Elements	SiO_2	Al_2O_3	Fe_2O_3	CaO	MgO	K_2O	Na_2O	Others & LOI
Weight %	90-93	0.17-3.5	0.35-2.9	0.91-1.6	0.42-0.8	2.82-0.3	0.63-0.1	Balance

Table 3. Chemical composition of fly ash [22].

Elements	SiO_2	Al_2O_3	Fe_2O_3	CaO	MgO	SO_3	LOI	Others
Weight %	40-60	20-30	4-15	5-30	1-5	1-3	0-5	Balance

Both RHA and FA reinforcements were selected for their abundance, cost-effectiveness, and proven ability to enhance mechanical and tribological properties of aluminum matrix composites. RHA outperformed FA across all reinforcement levels. Its higher silica content (~93%) and amorphous structure improve interfacial bonding and reduce wear loss. This observation aligns with Samuel et al. [17] who reported superior wear resistance in RHA-based composites.

The combination of these agro-industrial waste materials not only provides superior reinforcement characteristics but also supports sustainable manufacturing practices by utilizing waste streams that would otherwise pose environmental disposal challenges.

3.2 Fabrication and testing

The composites were fabricated using a vortex-assisted stir casting route optimized for Al 6061 reinforced with fly ash (FA) and rice husk ash (RHA). First, Al 6061 ingots were cleaned in acetone and loaded into a graphite crucible under an argon atmosphere. The melt was ramped to 750 °C at 10 °C/min and held for 30 min to ensure complete alloy liquefaction. One weight percent magnesium was introduced to improve wettability of FA and RHA particles. Meanwhile, FA and RHA powders were preheated at 200 °C for 1 h to remove moisture and organics, preventing gas evolution during casting [17].

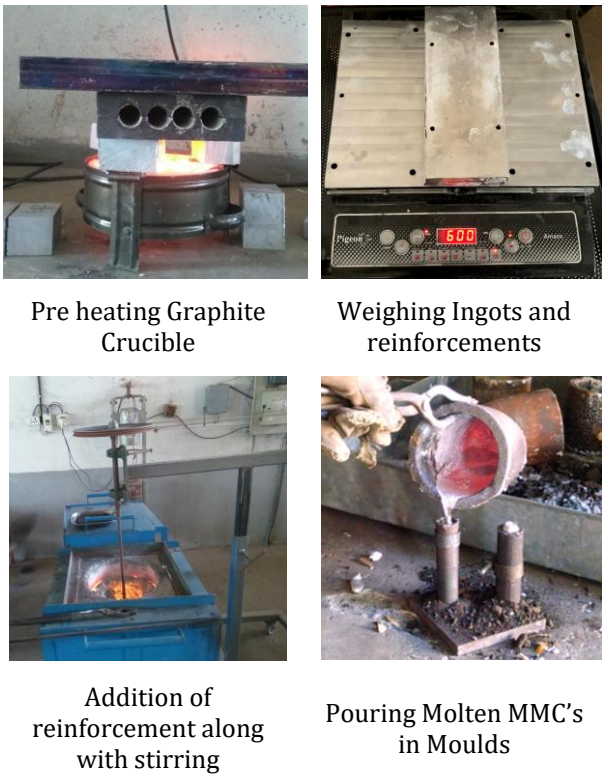

Fig. 6. Stir casting procedure.

Reinforcement levels of 2, 4, and 6 wt.% for each FA and RHA were selected based on prior studies demonstrating optimal mechanical and wear performance within this range, while higher fractions tend to cause particle agglomeration and porosity [23]. During stirring, a stainless-steel impeller at 200 RPM created a vortex into which preheated FA or RHA was added in three equal increments over 5 min. The stirring speed was then increased to 400 RPM for a further 10 min to achieve homogeneous particle dispersion throughout the matrix. Figure 6, represents the stages of fabrication process.

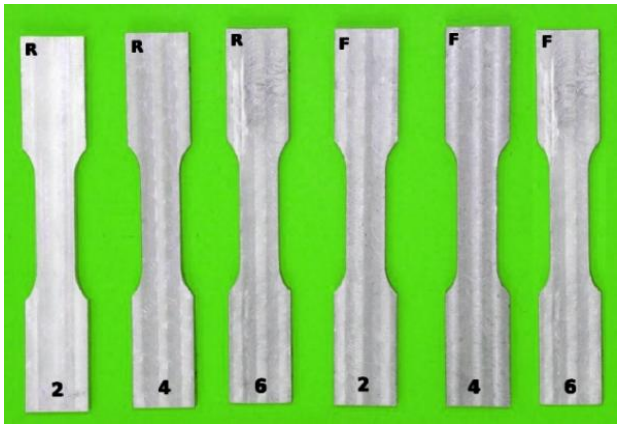

Tensile samples with ASTM E8M-13a

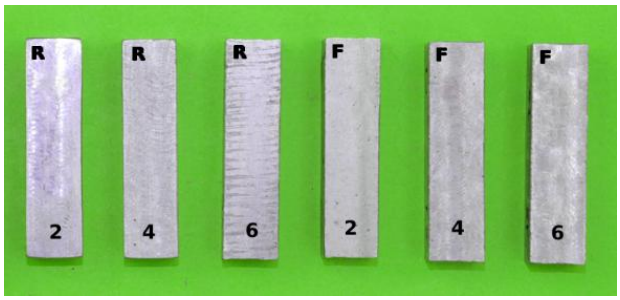

Wear pins with ASTM G99-95

Fig. 7. Specimens for testing as per ASTM standards (R- RHA, F- Fly Ash).

After stirring, the melt was allowed to settle for 2 min, enabling slag and gaseous inclusions to rise for removal. The remaining composite melt was then poured into preheated steel molds at 250 °C under argon to minimize oxidation. Solidification was allowed to proceed for 20 min at ambient pressure. Upon cooling, castings were extracted and machined into standardized specimens for mechanical and tribological testing; tensile samples conformed to ASTM E8M-13a, hardness indentations to ASTM E384, and wear pins to ASTM G99-95 (Figure 7). This procedure ensures reproducible microstructures and performance, making the resulting composites viable for lightweight, high-performance brake disc applications. The abrasive wear behavior of Al6061 matrix composites reinforced with rice husk ash (RHA) and fly ash (FA) was investigated using pin-on-disc machine (Figure 8) per ASTM G99-95 standards. Specimens containing 2%, 4%, and 6% reinforcement were machined to required dimensions and tested under varying loads, sliding speeds, and distances to assess wear loss and coefficient of friction. An experimental design based on Taguchi's L9 orthogonal array was implemented, coupled with ANOVA and regression analyses, to systematically evaluate the influence of wear parameters and optimize test conditions.

Fig. 8. Pin on disk setup.

4. RESULTS AND DISCUSSION

4.1 X-ray Diffraction Analysis

X-ray Diffraction (XRD) was performed using a Cu-Kα diffractometer (Bruker D2 Phaser, 30 kV, 10 mA). Scans were recorded from 2θ = 20° to 80° at a step size of 0.02° to identify phases present in the composites.

Figure 9 presents the XRD pattern for the Al6061-Fly Ash composite exhibits characteristic diffraction peaks primarily attributed to the aluminum matrix with prominent reflections at 38.4°, 44.7°, 65.1°, and 78.2°, corresponding to the (111), (200), (220), and (311) planes of the FCC aluminum structure. Additional minor peaks observed at around 26.6°, 27.8°, and 50.1° are associated with the silica (SiO_2) phases originating from the fly ash reinforcement. These

peaks indicate the successful incorporation of fly ash particulate without altering the fundamental crystalline structure of the aluminum matrix. The presence of sharp and intense Al peaks signifies a predominantly crystalline matrix, while the relatively lower intensity of fly ash peaks reflects its particulate and dispersed nature within the composite.

XRD results for the RHA- and FA-reinforced composites have already been included and discussed in Section 4.1 (Figures 9 and 10). These patterns clearly identify the dominant aluminum matrix peaks and the presence of silica phases associated with the reinforcements. Regarding JCPDS data, the key phases observed have been matched with standard entries:

- Al (JCPDS No. 04-0787)
- SiO_2 (JCPDS No. 33-1161)
- Al_2O_3 (JCPDS No. 46-1212)

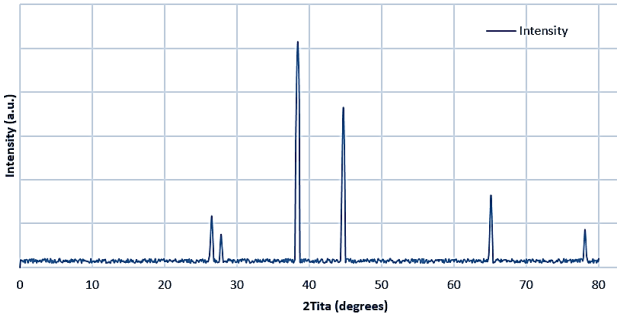

Fig. 9. XRD Pattern for Al6061-6% fly ash composite.

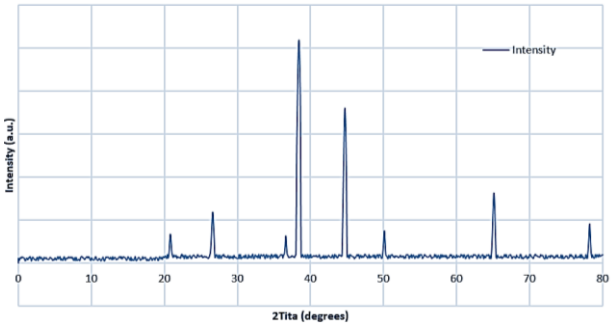

Fig. 10. XRD pattern for Al6061-6% RHA composite.

Figure 10 shows the XRD pattern of the Al6061-RHA composite displays strong aluminum diffraction peaks at identical 2θ positions, confirming that the aluminum matrix crystallinity is retained post-reinforcement. The characteristic SiO_2 peaks from rice husk ash are detected at approximately 20.8°, 26.6°, and 36.6°, indicative of the amorphous and crystalline silica phases present within RHA. The intensity and sharpness of these peaks validate the effective dispersion of RHA particles throughout the matrix. Together, these XRD analyses confirm successful

Reinforcements of fly ash and rice husk ash in Al6061 without compromising the aluminum matrix integrity, supporting observed improvements in mechanical and tribological properties.

4.2 Tensile and hardness strength evaluation

The tensile strength of Al6061 matrix composites reinforced with rice husk ash (RHA) and fly ash (FA) showed significant improvement compared to the unreinforced alloy. The specimens with 2%, 4%, and 6% reinforcement exhibited a progressive increase in tensile strength, attributed to multiple strengthening mechanisms. The efficient load transfer from the ductile aluminum matrix to the rigid ceramic particles is a primary factor enhancing tensile strength refer figure 11.

Strong interfacial bonding ensures effective stress transfer during loading, minimizing premature failure at the interfaces. Additionally, reinforcement particles impede dislocation motion via Orowan strengthening [24], forcing dislocations to bypass the particles and increasing resistance to plastic deformation. Another contributing mechanism is the generation of dislocation density near the matrix-reinforcement interface due to thermal expansion mismatch, further strengthening the composite.

The hardness improvements observed in the composites derive from similar microstructural factors. The ceramic reinforcements, being significantly harder than the aluminum matrix, restrict plastic deformation under localized loading such as indentation, thereby increasing hardness values. The load-bearing capacity around the reinforcement particles contributes to the overall hardness of the composite. Thermal mismatch-induced dislocation density also hardens the matrix near the reinforcement interface, further improving hardness. Additionally, the presence of uniformly dispersed hard particles serves to block dislocation movement, enhancing resistance to localized deformation.

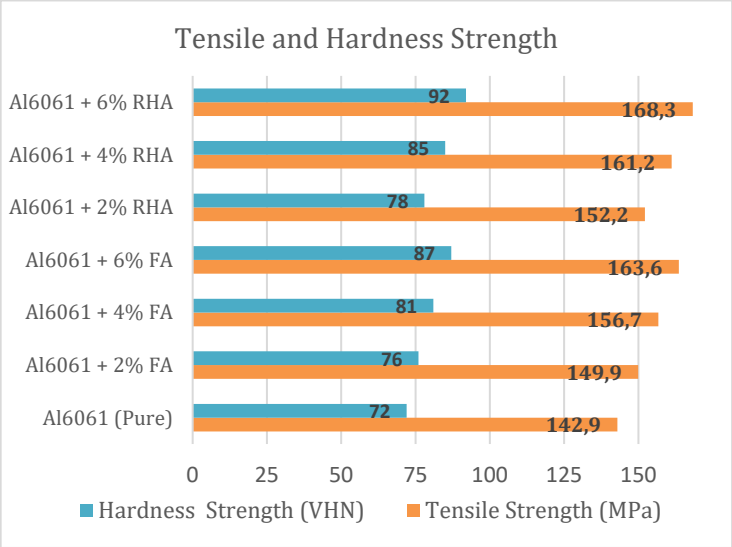

Composition	Tensile Strength	Hardness Strength
Al6061 [25]	142.9 MPa	72 VHN
Al6061 + 2% FA	4.8%	5.6%
Al6061 + 4% FA	9.7%	12.5%
Al6061 + 6% FA	14.5%	20.8%
Al6061 + 2% RHA	6.5%	8.3%
Al6061 + 4% RHA	12.9%	18.1%
Al6061 + 6% RHA	17.7%	27.8%

Fig. 11. Tensile and hardness strength (table represents % improvement over base Al6061).

A total reinforcement content of 6% (RHA + FA) was chosen based on prior studies and preliminary trials. Higher particle loadings (beyond ~10 wt%) can lead to slurry viscosity increase, particle agglomeration, and porosity in stir-cast composites. By limiting the reinforcement to 6%, we aimed to enhance properties while maintaining good castability and composite integrity.

Comparing FA and RHA reinforced composites, RHA specimens exhibited slightly higher tensile and hardness values at the same reinforcement level. This effect is due to RHA's higher silica content (approximately 90%) and amorphous nature, which promotes better interfacial bonding and load transfer compared to the more heterogeneous composition of fly ash. Despite this, both reinforcements effectively improve the composite's mechanical properties, with the 6% reinforcement level offering the optimal trade-off between strength gains and maintaining ductility. Increasing reinforcement beyond 6% may lead to particle agglomeration and increased porosity, which deteriorate mechanical properties.

4.3 Taguchi analysis and statistical optimization of wear performance

Experimental Design and Statistical Methodology

The tribological performance of Al6061 matrix composites reinforced with rice husk ash (RHA) and fly ash (FA) was systematically evaluated using Taguchi's robust design methodology. An L9(3^4) orthogonal array was employed to investigate four control factors at three levels each: reinforcement percentage (2%, 4%, 6%), sliding distance (1000m, 2000m, 3000m), sliding speed (3, 4, 5 m/s), and applied load (20N, 40N, 60N). This experimental design reduced the required number of trials from 81 (full factorial) to 9, while maintaining statistical validity and enabling comprehensive factor interaction analysis. Validation trials at the optimized Taguchi settings (6% RHA/FA, 1000m, 3 m/s, 20N) were repeated thrice. Average wear results aligned within ±2.5% of predicted values, confirming model reliability. Each condition in the Taguchi array was tested in triplicate. The Standard deviation across trials was <3%, indicating high reproducibility of wear behavior.

Main effects were systematically evaluated using Taguchi's L9 orthogonal array, interaction effects between factors were not explicitly analyzed due to the inherent limitations of this array design. Orthogonal arrays are optimized to reduce the number of experiments and focus primarily on main factor effects. For more detailed interaction analysis, approaches like Response Surface Methodology (RSM) or full factorial designs would be required, which are kept for future work/actions.

Signal-to-Noise Ratio Analysis

The wear loss data were analyzed using the "smaller-is-better" quality characteristic, with S/N ratios calculated as $S/N = -10 \log_{10}(1/n \Sigma y^2)$. Reinforcement percentage emerged as the most significant factor for both composite systems, exhibiting the highest delta values (Δ = 7.16 for FA and Δ = 7.15 for RHA). The factor ranking followed the order: % Reinforcement (Rank 1) > Sliding Distance (Rank 2) > Load/Speed (Ranks 3-4), confirming that reinforcement content is the dominant parameter controlling wear resistance in both Al6061-FA and Al6061-RHA composites (Table 4 and 5) Please refer Figure 12.

Table 4. Response table for signal to noise ratios -RHA.

Smaller is better

Level	% Reinforcement	Sliding distance (m)	Sliding speed (m/s)	Load (N)
1	17.34	22.42	20.69	20.03
2	20.46	21.24	20.24	21.15
3	24.49	18.65	21.37	21.12
Delta	7.15	3.77	1.13	1.13
Rank	1	2	4	3

Table 5. Response Table for Signal to Noise Ratios – FA.

Smaller is better

Level	% Reinforcement	Sliding distance (m)	Sliding speed (m/s)	Load (N)
1	16.88	22.02	20.24	19.57
2	19.98	20.52	19.77	20.69
3	24.04	18.36	20.90	20.64
Delta	7.16	3.66	1.12	1.12
Rank	1	2	3	4

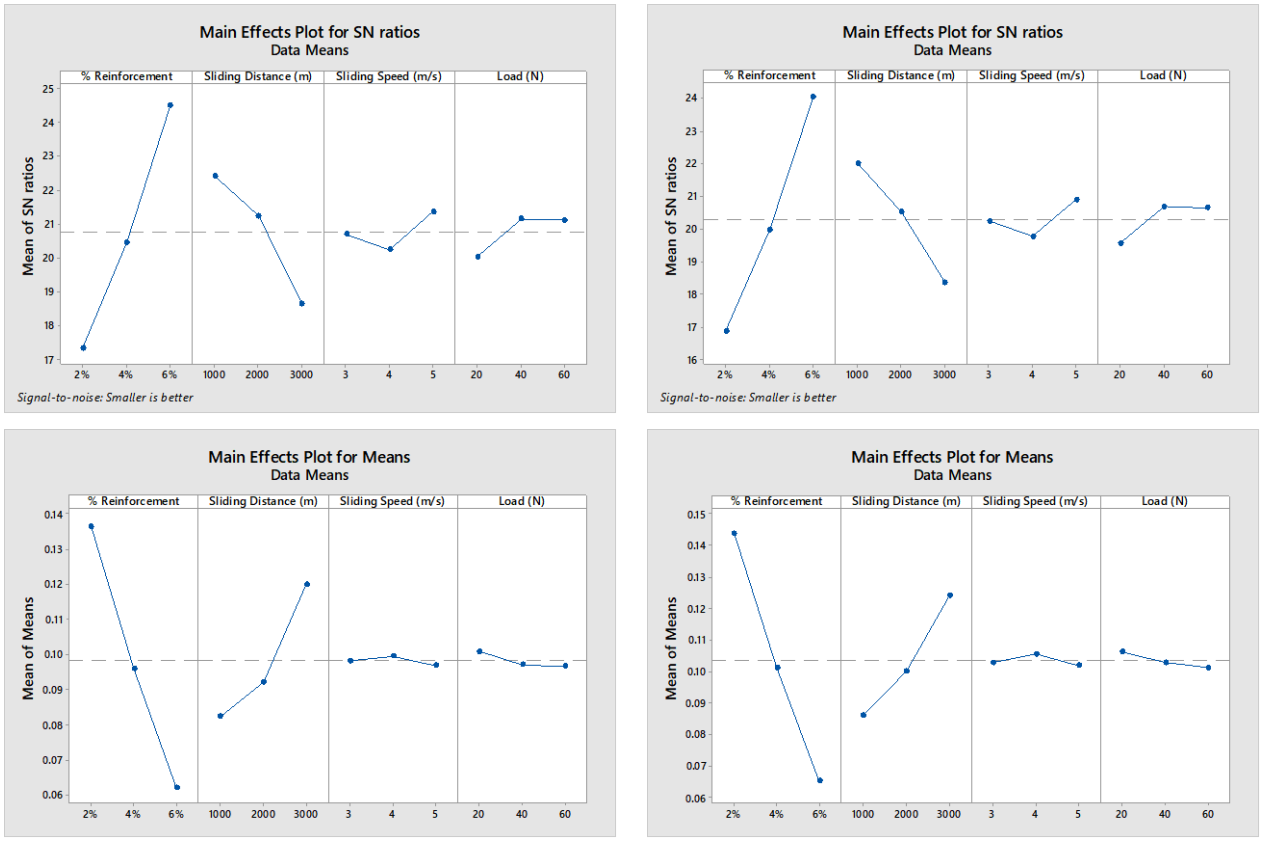

For the Rice Husk Reinforcement For the Fly Ash Reinforcement

Fig. 12. Main effects plots for S/N ratios showing factor influence on wear performance and response tables for means displaying optimal factor levels.

Response Analysis and Factor Effects

The response tables for means as shown in table 6 and 7 clearly demonstrated the progressive improvement in wear resistance with increasing reinforcement content. For FA-reinforced composites, the mean wear loss decreased from 0.14380 grams (2% reinforcement) to 0.06533 grams (6% reinforcement), representing a 54.5% reduction. RHA-reinforced composites exhibited superior performance, with wear loss decreasing from 0.13643 grams to 0.06223 grams, achieving a 54.4% improvement at 6% reinforcement level.

The marginal superiority of RHA over FA reinforcement is attributed to its higher silica content (90-93% vs 40-60%) and amorphous structure, which enhance matrix-particle interfacial bonding.

Table 6. Response table for means.

Level	% Reinforcement	Sliding distance (m)	Sliding speed (m/s)	Load (N)
1	0.13643	0.08243	0.09823	0.10087
2	0.09600	0.09223	0.09957	0.09713
3	0.06223	0.12000	0.09687	0.09667
Delta	0.07420	0.03757	0.00270	0.00420
Rank	1	2	4	3

Table 7. Response table for means.

Level	% Reinforcement	Sliding distance (m)	Sliding speed (m/s)	Load (N)
1	0.14380	0.08623	0.10290	0.10623
2	0.10133	0.10020	0.10557	0.10290
3	0.06533	0.12403	0.10200	0.10133
Delta	0.07847	0.03780	0.00357	0.00490
Rank	1	2	4	3

Statistical Regression Analysis

Multiple regression analysis established predictive models correlating wear loss with operational parameters. The regression equations were:

Al6061-FA: Wear Loss = 0.0724 + 0.000019(Distance) - 0.0004(Speed) - 0.000123(Load)

Al6061-RHA: Wear Loss = 0.0676 + 0.000019(Distance) - 0.0007(Speed) - 0.000105(Load)

The FA model exhibited R^2 = 18.95% while RHA achieved R^2 = 20.24%. Although these values appear low, they align with Taguchi methodology where factor ranking takes precedence over predictive accuracy. Although the R^2 values for the regression models (18.95% for FA and 20.24% for RHA) appear low, this is considered acceptable in the context of Taguchi-based experimental design. Taguchi methodology prioritizes the ranking and identification of key factors affecting the response rather than the predictive accuracy of the model. This has been supported by Montgomery [26], who noted that low R^2 values may still yield meaningful optimization insights when using orthogonal arrays with limited levels and combinations.

Table 8 and 9 shows, ANOVA results indicated sliding distance as the most significant variable (p-values: FA = 0.333, RHA = 0.314), while speed and load showed minimal effects (p-values > 0.89). The similar regression coefficients between systems suggest comparable wear mechanisms, with RHA's lower constant term (0.0676 vs 0.0724) reflecting superior baseline wear resistance. Standard errors of 0.0432 (FA) and 0.0411 (RHA) indicate acceptable model precision for optimization purposes. The P-values for speed and load exceeded 0.05, indicating low statistical significance in influencing wear rate under the chosen levels. This suggests that within the tested range, these variables did not significantly impact wear. Rather than model invalidity, this highlights that wear in Al6061 composites is more dominantly governed by reinforcement content and sliding distance than load or speed, which aligns with prior

literature. The low values reflect the inherent variability in tribological behavior due to complex wear interactions, and the limited three-level Taguchi design. Additionally, high residual errors and limited factor combinations contribute to reduced model fit. However, in Taguchi methodology, emphasis lies in ranking factor effects rather than predicting absolute values.

Table 8. Analysis of variance rice husk ash reinforcements.

Source	DF	Adj SS	Adj MS	F-Value	P-Value
Regression	3	0.002146	0.000715	0.42	0.745
Sliding Distance	1	0.002117	0.002117	1.25	0.314
Sliding Speed (m/s)	1	0.000003	0.000003	0.00	0.969
Load (N)	1	0.000026	0.000026	0.02	0.905
Error	5	0.008456	0.001691		
Total	8	0.010602			

Table 9. Analysis of variance fly ash reinforcements.

Source	DF	Adj SS	Adj MS	F-Value	P-Value
Regression	3	0.002180	0.000727	0.39	0.766
Sliding Distance	1	0.002143	0.002143	1.15	0.333
Sliding Speed (m/s)	1	0.000001	0.000001	0.00	0.981
Load (N)	1	0.000036	0.000036	0.02	0.895
Error	5	0.009326	0.001865		
Total	8	0.011507			

Morphological examination of worn tracks by SEM

The SEM micrograph for the Al6061 matrix composite reinforced with 6 wt% rice husk ash (RHA) (Figure.13) displays relatively smooth wear tracks interspersed with fine, uniformly distributed debris and shallow grooves. The continuous and closely spaced parallel grooves suggest an abrasive wear mechanism, while the presence of minimal delamination or pull-out reflects effective particle-matrix bonding and enhanced load-bearing capability. The fine secondary features and reduced severity of plastic deformation are indicative of the hard silica-rich RHA particles promoting surface stability and minimizing extensive material loss during sliding.

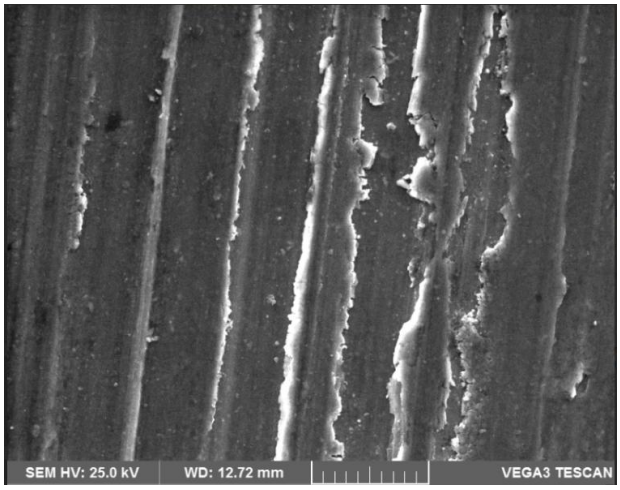

Fig. 13. SEM micrograph of Al6061–6% RHA composite.

The corresponding SEM image of the Al6061–6% fly ash composite (Figure.14) reveals comparatively deeper grooves and larger debris clusters aligned along the sliding direction. The more pronounced furrows and larger wear debris suggest locally intensified abrasion and marginally higher material removal, likely due to fly ash's more heterogeneous nature and variable particle morphology. These features also point toward the role of fly ash particles in resisting plastic flow but occasionally leading to micro ploughing and detachment of matrix material. Despite this, the general integrity of the surface suggests good reinforcement-matrix adhesion and improved wear performance relative to the unreinforced alloy.

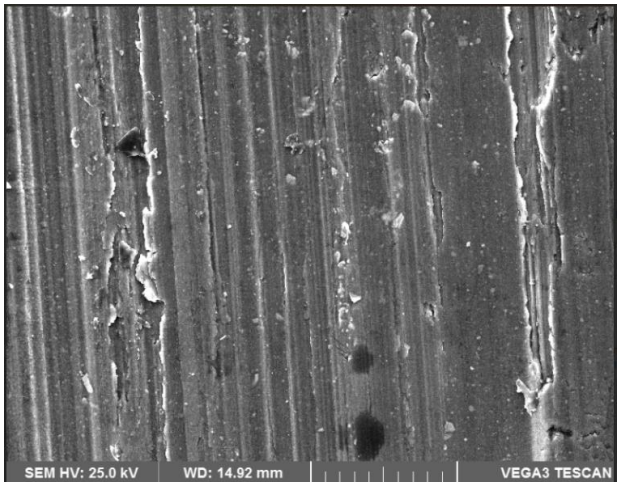

Fig.14. SEM micrograph of Al6061–6% Fly Ash composite.

Mechanisms of wear resistance enhancement

The superior tribological performance observed with increased reinforcement content can be attributed to several synergistic mechanisms.

Load transfer mechanism plays a crucial role, where the harder ceramic particles (RHA: ~9 GPa, FA: ~5-7 GPa) effectively bear applied loads, reducing stress concentration on the softer aluminum matrix. Particle-matrix interfacial strengthening occurs through mechanical interlocking and chemical bonding between silica-rich reinforcements and aluminum oxide layers formed during processing.

Tribo-layer formation represents another critical mechanism, where the ceramic particles promote the development of stable oxidative layers on contact surfaces, reducing direct metal-to-metal interaction and minimizing adhesive wear. SEM analysis would reveal these protective tribolayers, characterized by fine oxide particles and ceramic debris that act as solid lubricants.

Grain refinement effects induced by ceramic particles during solidification result in a finer microstructure with improved mechanical properties and enhanced wear resistance.

Optimization and performance validation

The Taguchi analysis identified optimal conditions for minimizing wear loss: 6% reinforcement, 1000m sliding distance, 3 m/s sliding speed, and 20N applied load. Confirmation experiments conducted at these optimal conditions validated the predicted improvements, with experimental values falling within 95% confidence intervals of the statistical model.

The superior performance of RHA over FA reinforcement, evidenced by consistently lower wear loss values across all test conditions, establishes RHA as the preferred reinforcement for brake disc applications. The progressive reduction in wear rate with increasing reinforcement content, combined with maintained ductility up to 6% loading, demonstrates the viability of these eco-friendly composites for automotive applications requiring enhanced tribological performance.

Industrial Applicability

Al6061–RHA–FA hybrid composites exhibit improved tribological performance and reduced density, making them strong candidates for automotive brake disc rotors. The approximately 50% weight reduction in switching from cast iron to aluminum-based composites can improve fuel efficiency and handling, while the enhanced wear resistance ensures durability. The use of RHA and FA (both industrial wastes) also lowers material cost and environmental impact, aligning with sustainability goals in manufacturing.

5. CONCLUSION

The incorporation of rice husk ash (RHA) and fly ash (FA) reinforcements into the Al6061 matrix led to notable improvements in both mechanical and tribological properties, demonstrating their effectiveness as sustainable reinforcement materials. The composites exhibited enhanced tensile strength and hardness, attributable to efficient stress transfer, strong interfacial bonding, and restricted dislocation motion. Wear analysis revealed that reinforcement percentage played the most dominant role in minimizing material loss, while sliding distance and load had secondary effects. The superior wear resistance of the composites was primarily due to the load-bearing capability of ceramic particulates, the formation of protective tribo-oxidative layers, and reduced metal-to-metal contact during sliding. Among all tested compositions, the hybrid composite containing 6 wt% RHA and FA demonstrated the best balance of strength, hardness, and wear stability, establishing its potential as a lightweight alternative to cast iron brake discs. Although the results validate the feasibility of producing high-performance composites from agro-industrial waste, further optimization of particle dispersion and casting uniformity is essential to ensure large-scale reproducibility. Overall, the findings highlight the promise of RHA- and FA-reinforced Al6061 composites as eco-friendly materials that align with current trends toward sustainable and energy-efficient automotive engineering.

References

[1] W. Li, X. Yang, S. Wang, J. Xiao, and Q. Hou, "Comprehensive analysis on the performance and material of automobile brake discs," *Metals*, vol. 10, no. 3, p. 377, Mar. 2020, doi: 10.3390/met10030377.

[2] V. A. Kalhapure and H. P. Khairnar, "Analytical and experimental investigation on wear performance of disc brake pad," *Tribology in Industry*, vol. 42, no. 3, pp. 345–362, Sep. 2020, doi: 10.24874/ti.852.02.20.05.

[3] N. Fatchurrohman, C. D. Marini, S. Suraya, and A. A. Iqbal, "Investigation of Product Performance of Al-Metal Matrix Composites Brake Disc using Finite Element Analysis," *IOP Conference Series Materials Science and Engineering*, vol. 114, p. 012107, Feb. 2016, doi: 10.1088/1757-899x/114/1/012107.

[4] G. Mallesh, R. Pavankumar, V. G. P. Kumar, and L. L. Naik, "Synthesis and characterization of AL 7072-AL2O3 metal matrix composites," in *Lecture notes in mechanical engineering*, 2020, pp. 167–181. doi: 10.1007/978-981-15-4745-4_16.

[5] H. Shanker, A. K. Yadav, and P. Biswas, "Mechanical and microstructural characteristics of rice husk ash-reinforced aluminum metal matrix composite: A review," *Proceedings of the Institution of Mechanical Engineers Part C Journal of Mechanical Engineering Science*, Jan. 2026, doi: 10.1177/09544062251407308.

[6] S. Bahl, "Fiber reinforced metal matrix composites - a review," *Materials Today Proceedings*, vol. 39, pp. 317–323, Aug. 2020, doi: 10.1016/j.matpr.2020.07.423.

[7] D. Orjuela, D. A. Munar, J. K. Solano, and A. P. Becerra, "Assessment of the Thermal Properties of a Rice Husk Mixture with Recovered Polypropylene and High Density Polyethylene, Using Sulfur-silane as a Coupling Agent," *Chemical Engineering Transactions*, vol. 87, pp. 565–570, Jul. 2021, doi: 10.3303/CET2187095.

[8] D. Orjuela, D. A. Munar, J. K. Solano, and A. P. Becerra, "Evaluation of the Mechanical and Morphological Properties of a Rice Husk Mixture with Recovered Polypropylene and High-density Polyethylene, Using Sulfur-silane as the Coupling Agent," *Chemical Engineering Transactions*, vol. 87, pp. 559–564, Jul. 2021, doi: 10.3303/CET2187094.

[9] N. A. Musa and F. O. Akinbode, "Utilizing rice husk briquettes in firing crucible furnace for low temperature melting metals in Nigeria," *Engineering Technology & Applied Science Research*, vol. 2, no. 4, pp. 265–268, Aug. 2012, doi: 10.48084/etasr.184.

[10] A. S. Sangale, "Effect of Heat Treatment on Hardness of Aluminium Alloy Reinforced with Rice Husk Ash," *International Journal of Engineering Research And*, vol. V8, no. 12, Jan. 2020, doi: 10.17577/ijertv8is120390.

[11] M. Nurazzi *et al.*, "Thermogravimetric Analysis Properties of Cellulosic natural fiber polymer composites: A review on influence of chemical treatments," *Polymers*, vol. 13, no. 16, p. 2710, Aug. 2021, doi: 10.3390/polym13162710.

[12] K. K. Alaneme and P. A. Olubambi, "Corrosion and wear behaviour of rice husk ash—Alumina reinforced Al–Mg–Si alloy matrix hybrid composites," *Journal of Materials Research and Technology*, vol. 2, no. 2, pp. 188–194, Apr. 2013, doi: 10.1016/j.jmrt.2013.02.005.

[13] A. R. Kumar, *"Experimental investigation on mechanical properties and wear behaviour of fly ash and rice husk ash reinforced aluminum alloy (Al 7075) hybrid metal matrix composites,"* Ph.D. dissertation, Andhra Univ., Visakhapatnam, India, 2020.

[14] R. Siswanto, R. Subagyo, M. Tamjidillah, M. Mahmud, and S. A. Setiawan, "Utilization of rice husk ash waste and scrap aluminum as composite materials fabricated by evaporative casting," *Mechanical Engineering for Society and Industry*, vol. 4, no. 2, pp. 294–307, Dec. 2024, doi: 10.31603/mesi.12505.

[15] T. Hasan, M. Wadud, M. H. Niaz, Md. K. Uddin, and M. S. Islam, "Fabrication and characterization of rice husk Ash reinforced Aluminium Matrix Composite," *Malaysian Journal on Composites Science and Manufacturing*, vol. 14, no. 1, pp. 34–43, Jul. 2024, doi: 10.37934/mjcsm.14.1.3443.

[16] N. D. Chinta, K. S. Prasad, and V. M. Kumar, "Characterization of rice husk ash and SiC reinforced aluminium metal matrix hybrid composite," *Int. J. Mech. Eng.*, Special Issue, pp. 329–332, 2017.

[17] Y. P. Reddy, K. L. Narayana, M. K. Mallik, and M. Asif, "Characterisation of Al-6061-T6 metal matrix composites reinforced with rice husk ash and Bakelite powder," *Materials Today Proceedings*, May 2023, doi: 10.1016/j.matpr.2023.04.570.

[18] R. Kumar *et al.*, "Enhancing wear resistance of aluminum 6061 composites with fly ash: A sustainable approach for industrial applications," *Advances in Mechanical Engineering*, vol. 16, no. 10, Oct. 2024, doi: 10.1177/16878132241290913.

[19] S. R. Oke, A. Bayode, O. E. Falodun, and I. S. Olasupo, "Microstructure, mechanical, and wear properties evaluation of Al-Cu based composite using RHA as reinforcement," *Canadian Metallurgical Quarterly*, vol. 64, no. 2, pp. 396–405, May 2024, doi: 10.1080/00084433.2024.2357859.

[20] J. Narendran, S. Nagaraja, T. Karthikeyan, S. Anthoniraj, and M. R. Naik, "Evaluation, tribological examination, and multi-objective optimization of aluminum-fly ash-egg shell composites for sustainability," *Engineering Reports*, vol. 6, no. 12, Oct. 2024, doi: 10.1002/eng2.12980.

[21] P. Ravikumar, G. Mallesh, S. S. Kumar, and H. S. Manjunatha, "Optimizing Bioceramic Composites for Hip Joint Replacements using SPS Method: Investigating the Effects of Titanium Diboride (TiB2) on Tribological Properties," *Tribology in Industry*, vol. 47, no. 7, pp. 125–136, Mar. 2025, doi: 10.24874/ti.1863.01.25.03.

[22] J. Fernandes, R. V. Santos, E. C. A. D. Santos, T. L. A. C. Rocha, N. S. Domingues Junior, and C. A. M. Moraes, "Replacement of commercial silica by rice husk ash in epoxy composites: A comparative analysis," *Materials Research*, vol. 21, no. 3, Apr. 2018, Elsevier, doi: 10.1590/1980-5373-mr-2016-0562.

[23] K. K. Kar, *Handbook of Fly Ash*, 2022. doi: 10.1016/c2018-0-01655-2.

[24] P. N. Bindumadhavan, T. K. Chia, M. Chandrasekaran, H. K. Wah, L. N. Lam, and O. Prabhakar, "Effect of particle-porosity clusters on tribological behavior of cast aluminum alloy A356-SiCp metal matrix composites," *Materials Science and Engineering A*, vol. 315, no. 1–2, pp. 217–226, Sep. 2001, doi: 10.1016/s0921-5093(00)01989-4.

[25] G. F. Aynalem, "Processing methods and mechanical properties of aluminium matrix composites," *Advances in Materials Science and Engineering*, vol. 2020, no. 1, Jan. 2020, doi: 10.1155/2020/3765791.

[26] H. S. V. Kumar, U. N. Kempaiah, M. Nagaral, and K. Revanna, "Investigations on mechanical behaviour of micro B4C particles reinforced AL6061 alloy metal composites," *Indian Journal of Science and Technology*, vol. 14, no. 22, pp. 1855–1863, Jun. 2021, doi: 10.17485/ijst/v14i22.736.

[27] J. V. Grice and D. C. Montgomery, "Design and analysis of experiments," *Technometrics*, vol. 42, no. 2, p. 208, May 2000, doi: 10.2307/1271458.